Influence of P450 3A4 SRS-2 Residues on Cooperativity and/or Regioselectivity of Aflatoxin B_1 Oxidation

Linlong Xue,[†] Huifen Faye Wang,[†,‡] Qinmi Wang,[§] Grazyna D. Szklarz,[||] Tammy L. Domanski,[§] James R. Halpert,[§] and Maria Almira Correia*[,†]

Departments of Cellular and Molecular Pharmacology, Pharmaceutical Chemistry, and Biopharmaceutical Sciences and the Liver Center, University of California, San Francisco, California 94143, Department of Basic Pharmaceutical Sciences, School of Pharmacy, West Virginia University, Morgantown, West Virginia 26506, and Department of Pharmacology and Toxicology, University of Texas Medical Branch, Galveston, Texas 77555-1031

Received October 12, 2000

The major human liver drug-metabolizing cytochrome P450 enzymes P450 3A4 and P450 3A5 share >85% amino acid sequence identity yet exhibit different regioselectivity toward aflatoxin B_1 (AFB_1) biotransformation [Gillam et al. (1995) *Arch. Biochem. Biophys.* **317**, 74−384]. P450 3A4 prefers AFB1 3α-hydroxylation, which detoxifies and subsequently eliminates the hepatotoxin, over AFB1 *exo*-8,9-oxidation. P450 3A5, on the other hand, is a relatively sluggish 3α-hydroxylase and converts AFB_1 predominantly to the genotoxic *exo*-8,9-epoxide. Using a combination of approaches (sequence alignment, homology modeling and site-directed mutagenesis), we have previously identified several divergent residues in four of the six putative substrate recognition sites (SRSs) of P450 3A4, which when replaced individually with the corresponding amino acid of P450 3A5, resulted in a significant switch of the characteristic P450 3A4 AFB_1 regioselectivity toward that of P450 3A5 [Wang et al. (1998) *Biochemistry* **37**, 12536−12545]. In particular, residues N206 and L210 in SRS-2 were found to be critical for AFB_1 detoxification via 3α-hydroxylation, and the corresponding mutants N206S and L210F most closely mimicked P450 3A5, not only in its regioselectivity of AFB_1 metabolism but also in its overall functional capacity. We have now further explored the plausible reasons for such relative inactivity of the SRS-2 mutants by examining N206S and additional mutants (L210A, L211F, L211A, and N206E) and found that the dramatically lowered activities of the N206S mutant are accompanied by a loss of cooperativity of AFB_1 oxidation. Molecular dynamics analyses with an existing P450 3A4 homology model [Szklarz and Halpert (1997) *J. Comput. Aided Mol. Des.* **11**, 265] suggested that N206 (helix F) interacts with E244 (helix G), creating a salt bridge that stabilizes the protein structure and/or defines the active site cavity. To examine this possibility, several E244 mutants (E244A, V, N, S) were tested, of which E244S was the most notable for its relatively greater impairment of P450 3A4-dependent AFB_1 3α-hydroxylation. However, the results with these E244 mutants failed to validate the N206−E244 interaction predicted from these molecular dynamics analyses. Collectively, our findings to date have led us to reconsider our original interpretations and to reexamine them in the light of AFB_1 molecular modeling analyses with a newly refined P450 3A4 homology model. These analyses predicted that F304 in SRS-4 (I-helix) plays a pivotal role in AFB_1 binding at the active site in either orientation leading to 3α- or *exo*-8,9-oxidation. Consistent with this prediction, conversion of F304 to Ala abolished P450 3A4-dependent AFB_1 3α-hydroxylation and *exo*-8,9-oxidation.

The cytochromes P450 (P450s)[1] play important roles not only in the biosynthesis of endobiotics, but also in the metabolic detoxification and/or bioactivation of natural and foreign chemicals that include drugs, toxins, and carcinogens (*1*−*3*). P450s 3A4 and 3A5 are the dominant enzymes in the adult human liver that are responsible for the metabolism of over 60% of clinically relevant drugs (*4*−*7*). Examination of the metabolic capacity of P450 3A4, the major human liver P450, has led to its characterization as an unusually versatile catalyst, with an active site capable of not only accepting very large as well as small sized substrates, but also accommodating more than one substrate molecule at a time, thereby resulting in homotropic and/or heterotropic cooperativity[2]

* To whom correspondence should be addressed. Phone: (415) 476-3992. Fax: (415) 476-5292. E-mail: mariac@itsa.ucsf.edu.
[†] University of California.
[‡] Present address: Pfizer Inc., Groton, CT.
[§] University of Texas Medical Branch.
[||] West Virginia University.

[1] Abbreviations: AFB_1, Aflatoxin B_1; AFQ_1, 3α-hydroxy AFB_1; ALA, δ-aminolevulinic acid; b_5, cytochrome b_5; CHAPS, (3-[(3-cholamidopropyl)dimethylammonio]-1-propane-sulfonate; P450s, CYPs, cytochromes P450; DETAPAC, diethylenetriaminepentaacetic acid; PCR, polymerase chain reaction.

[2] Homotropic cooperativity involves interactions between a substrate and one or more effector molecules of identical chemical structure, whereas heterotropic cooperativity involves corresponding interactions between a substrate and effector molecules of different chemical structure.

10.1021/tx000218z CCC: $20.00
Published on Web 04/06/2001

Scheme 1. P450 3A4-Dependent Oxidation of AFB_1 to the 3α-Hydroxy (AFQ_1) Product and *exo*-8,9-Epoxide

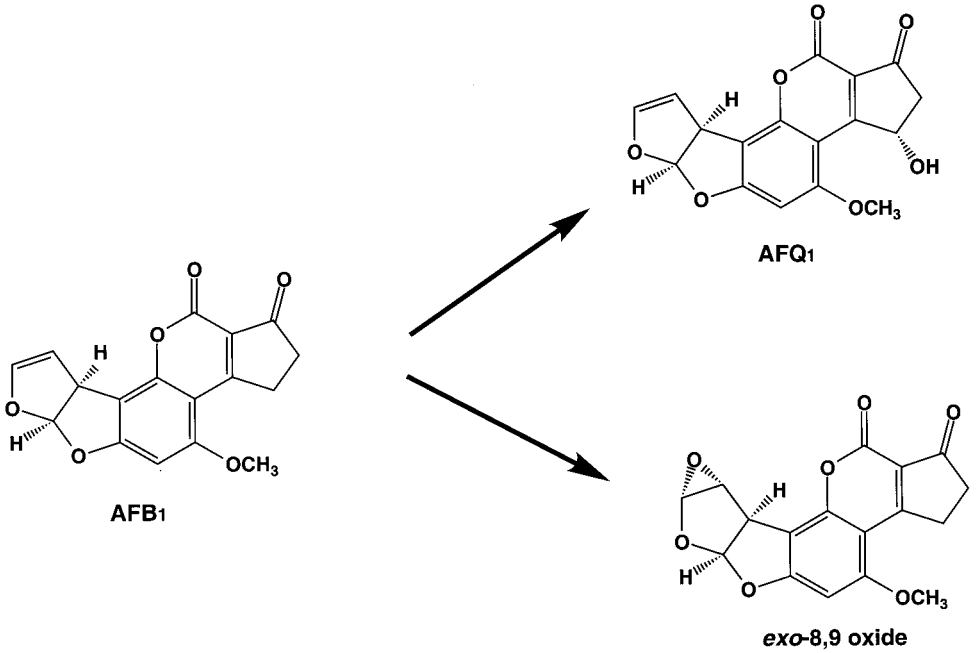

(*8*−*16*). On the other hand, P450 3A5 represents a polymorphic form representing up to 100% of P4503A content in 25−30% of adult human livers (*17*, *18*). Although these two P450s share >85% amino acid sequence identity, they exhibit striking functional differences in their catalytic preference of certain substrates and in their regioselectivity toward aflatoxin B_1 (AFB_1) biotransformation (*18*−*22*; Scheme 1). Accordingly, while P450 3A4 apparently prefers AFB_1 3α−hydroxylation (to form AFQ_1) which detoxifies and subsequently eliminates the hepatotoxin, over AFB_1 *exo*-8,9-oxidation, P450 3A5 is incapable of appreciable AFB_1 3α-hydroxylation and converts it predominantly to the genotoxic *exo*-8,9-oxide (*9*, *21*−*23*). In an attempt to elucidate the structural features that govern the differential regioselectivity of the human liver 3A enzymes in AFB_1 metabolism and bioactivation, we employed a combination of approaches (sequence alignment, homology modeling, and site-directed mutagenesis) to examine whether substitution of a single amino acid in one of the six putative *substrate recognition sites* (SRSs) of P450 3A4 with the corresponding amino acid of P450 3A5 would switch its regioselectivity (*23*). Of the 3A4 mutants examined, P107S, F108L, N206S, L210F, V376T, S478D, and L479T exhibited a significant switch of P450 3A4 regioselectivity toward that of P450 3A5 (*23*). The results confirmed the importance of some of these residues for substrate contact/orientation in the active site with residues N206 and L210 (SRS-2) being critical for AFB_1 detoxification via 3α-hydroxylation (*23*). Furthermore, the 3A4 mutants N206S and L210F most closely mimicked P450 3A5 in their regioselectivity of AFB_1 metabolism and in their overall functional capacities as defined by relatively low metabolic ratios of AFQ_1/*exo*-8,9-oxide, thereby revealing that *a single 3A5 SRS domain* (*SRS-2*) *was capable of conferring the 3A5 phenotype on 3A4* (*23*). We have extended this finding by examining the specific effect of the replacement of N206 on the catalytic acceptance and consequently the observed AFB_1 cooperativity and/or regioselectivity at the P450 3A4 active site. We also probed whether substitution of other P450 3A4 SRS-2 residues (L210 and L211) known to be involved in heterotropic substrate-effector interactions and/or substrate specificity of testosterone and progesterone, two well recognized P450 3A4 steroid substrates (*10*−*12*, *16*), would similarly affect AFB_1 regioselectivity. These residues are highly conserved in all P450 3A subfamily members examined to date, except P450 3A5 which contains a Phe residue instead of Leu at position 210. Our findings described below have led us to reconsider how these residues might be affecting AFB_1-active site interactions and to revise our original hypothesis on the basis of a refined P450 3A4 homology model.

Experimental Procedures

Materials. Testosterone and its hydroxylated metabolites, AFB_1, AFQ_1, δ-aminolevulinic acid (ALA), NADPH, GSH (reduced form), sodium cholate, catalase, 3-[(3-cholamidopropyl)-dimethylammonio]-1-propane-sulfonate (CHAPS), lysozyme, diethylenetriaminepentaacetic acid (DETAPAC), and purified rat liver GSH S-transferase (GST) were obtained from Sigma (St. Louis, MO). L-α-dilauroylphosphatidylcholine, L-α-dioleyl-*sn*-glycerophosphatidylcholine, and phosphatidylserine were purchased from Doosan Serdary Research Laboratories (Englewood Cliffs, NJ). DNase and RNase were purchased from Boehringer-Mannheim (Indianapolis, IN). Cytochrome b_5 (b_5) and cytochrome P450 reductase were purified from male rat liver microsomes according to previously reported methods (*24*). The GSH adduct of AFB_1 *exo*-8,9-oxide used as a standard was enzymatically synthesized, purified by HPLC and characterized spectrally as described previously (*25*). All other reagents were of the highest commercial purity.

Site-Directed Mutagenesis of P450 3A4. As previously (*23*), the cDNAs for P450s 3A4 and 3A5 engineered to code for deletions of the N-terminal residues 3−12 and substitution of residue Ser18 with Phe, and incorporated into the pCW vector were gifts from Dr. R. Estabrook (University of Texas, SW Med. School, Dallas, TX). The 3A4 cDNA was removed from the pCW vector and inserted into pBluescript KS+ for generation of some of the mutants. The Quick-change site-directed mutagenesis kit (Stratagene, La Jolla, CA) was used for the generation of the following mutants: N206S, N206E, E244N, E244A, E244S, and E244V. The oligonucleotide pairs for each mutant are listed in Table 1. Double mutant N206E/E244N was generated from

Table 1. List of Oligonucleotides and Restriction Enzymes Used for Screening Each P450 3A4 Mutation[a]

mutation	oligonucleotide primer[c]	restriction enzyme[d]
N206E	5′-CCC TTT GTG GAA GAG ACC AAG AAG C-3′ 5′-GCT TCT TGG TCT CTT CCA CAA AGG G-3′	*Ear*I (+)
E244N	5′-CTG TGT GTT TCC AAG GAA TGT TAC AAA TTT-3′ 5′-AAA TTT GTA ACA TTC CTT GGA AAC ACA CAG-3′	unique site for *Sty*I(+)
E244A	5′-CTG TGT GTT TCC AAG AGC GGT TAC AAA TTT TTT-3′ 5′-AAA AAA TTT GTA ACC GCT CTT GGA AAC ACA CAG-3′	*Brs*BI (+)
E244S	5′-GTG TGT TTC CAA GAA GCG TTA CAA ATT TTT TAA-3′ 5′-TTA AAA AAT TTG TAA CGC TTC TTG GAA ACA CAC-3′	*e*
E244V	5′-CTG TGT GTT TCC AAG AGT TGT TAC AAA TTT TTT AAG-3′ 5′-CTT AAA AAA TTT GTA ACA ACT CTT GGA AAC ACA CAG-3′	*e*
N206E/E244N[b]		*Ear*I (+)/*Sty*I(+)

[a] The sequence of each mutant was verified by DNA sequencing analyses. [b] No additional primers were employed. Instead, the E244N mutagenesis primers were used on the N206E template plasmid to get the target mutant. [c] The underlined nucleotides was/were altered to introduce the desired mutation. [d] (+, −) Gain or loss of indicated restriction site. [e] No restriction site was introduced.

Table 2. Regioselectivity of Testosterone and AFB_1 Hydroxylations by P450s 3A4, 3A5, and 3A4 Srs-2 Structural Mutants

		testosterone (T) hydroxylation[a] (nmol OH-T formed/nmol P450/min)			AFB_1 hydroxylation[b] (nmol AFB_1 metabolite formed/nmol P450/min)		
SRS domains	P450s	6β-OHT	2β-OHT	6β-/2β-OHT	AFQ_1	8,9-epoxide	AFQ_1/8,9-epoxide
	3A4wt	26.8 ± 3.91	1.85 ± 0.06	14.5	2.04 ± 0.32	0.80 ± 0.14	2.55
	3A5wt	4.55 ± 2.37	0.79 ± 0.22	5.76	0.02	0.06	0.33
SRS-2	N206S	1.66 ± 0.33	ND[c]		0.11 ± 0.05	0.35 ± 0.06	0.31
	L210F	27.4	1.54	17.8	0.15	0.33	0.45
	L210A	25.2	0.36	70	0.04	0.37	0.11
	L211F	30.1	3.38	8.9	0.19	0.69	0.28
	L211A	12.7	1.21	10.5	0.21	0.39	0.53
	N206S, K209M	ND	ND		ND	2.22	

[a] Values listed are mean ± SD of at least three individual determinations or the mean of two individual determinations. [b] AFQ_1 is the 3α-hydroxylated AFB_1 metabolite. 8,9-Epoxides were assayed by the combined yield of their GSH adducts and the diol species. Values listed are the mean ± SD of at least four individual determinations or the mean of at the least two individual determinations. [c] ND, nondetectable.

N206E with the use of the mutagenesis primers described to generate E244N. The double mutant N206S/K209M was generated accidentally in the course of construction of N206S, but proved functionally interesting and was included in our analyses. The mutated P450 3A4 cDNAs were subsequently transferred to the pCW expression vector using standard cloning techniques. The strategies for construction of mutants L210F, L210A, L211F, L211A, and F304A using the Expand High Fidelity PCR system (Boehringer-Mannheim, Indianapolis, IN) and the plasmid template pSE3A4His have been previously reported (*10*−*12*, *16*). Standard PCR conditions were used to generate the mutated cDNAs. All mutant plasmids were screened by restriction enzyme digestion and confirmed by DNA sequencing to confirm the presence of the desired mutations and to verify the absence of extraneous mutations.

Expression of Wild-Type (wt) P450s 3A4 and 3A5 and P450 3A4 Point-Mutants. The wild-type and mutant P450s 3A4 were expressed in *Escherishia coli* XL-1 blue cells, *E. coli* DH5αF′ cells, or *E. coli* Topp3 cells exactly as described previously (*23*). Bacterial cells were harvested at 20−26 h after induction.

CHAPS Solubilization of *E. coli*-Expressed P450s. Bacterial cell membranes were prepared and solubilized in the presence of protease inhibitors during solubilization exactly as described (*23*, *24*). The solubilized membranes were clarified by centrifugation at 100000*g* at 4 °C for 30 min, the supernatant was assayed for its P450 content by the method of Omura and Sato (*26*). The solubilized membrane fractions were aliquoted and stored at −80 °C until use. The authenticity of the expressed P450s as 3A proteins was verified by immunoblotting of the solubilized *E. coli*-membranes against polyclonal anti-P450 3A4 IgGs.

Testosterone Metabolism by Solubilized Recombinant Enzymes. Testosterone 6β- and 2β-hydroxylase activities of the solubilized P450 proteins functionally reconstituted with P450 reductase and/or b_5 were determined at a previously determined optimal molar ratio of P450 3A4:reductase:b_5 of 1:4:2 as described (*23*, *27*). Briefly the assay conditions were as follows with the reagents added at 4 °C in the following order: lipid mix (L-α-dilauroylphosphatidylcholine:L-α-dioleyl-*sn*-glycerophosphatidylcholine:phosphatidylserine, 1:1:1, w/w; 10 μg), sodium cholate (100 μg), b_5 (20 pmol), P450 reductase (40 pmol), P450 3A4 or mutant (10 pmol), and GSH (1.5 mmol). The above mix was reconstituted at room temperature for 10 min and then placed back in ice. The following reagents were then added in order: Hepes buffer (50 mM, pH 7.85), catalase (100 units), DETAPAC (1 mM), water (*q.s.* 0.5 mL), $MgCl_2$ (30 mM), and [^{14}C]testosterone (0.14 μCi; 0.25 mM). The mixture was preincubated at 37 °C for 2 min, and NADPH (1 mM) was added to start the reaction. The reaction was terminated with 1 mL of CH_2Cl_2. The metabolites were extracted twice with 2 mL of CH_2Cl_2, dried down under N_2, and assayed by HPLC with radioquantitation as described previously (*27*). The data listed in Table 3 were obtained from incubations containing only cold testosterone and the metabolites extracted without added carrier metabolites and subjected to HPLC with peak area quantitation for each hydroxylated metabolite. With the latter assay method, wild-type P450 3A4 gave comparable 2β- and 6β-hydroxytestosterone values to those obtained with the radioactive assay (Tables 2 and 3).

AFB_1 Metabolism by Recombinant P450s. The formation of 3α-hydroxyAFB_1 and AFB_1 *exo*-8,9-oxide (the only epoxide detected and assessed by the combined yields of its corresponding GSH-adduct and the diols) by native and mutant enzymes was assayed by the method of Ueng et al. (*28*) with the modifications to improve the enzyme activity and stability described previously (*23*). Lipid mix (L-α-dilauroyl-phosphatidylcholine:L-α-dioleyl-*sn*-glycerophosphatidylcholine:phosphatidylserine 1:1:1, w/w) was sonicated in water at a stock concentration of 0.5 μg/μL and stored at −20 °C. The following components were added in strict order: lipid mix (20 μg/mL), sodium cholate (200 μg/mL), b_5 (200 pmol), P450 reductase (400 pmol), solubilized bacterial membrane P450s (100 pmol), and GSH (3 mM). The mixture was incubated at room temperature followed by the addition of water, Hepes buffer (50 mM, pH 7.85), catalase (200 units/mL), DETAPAC (1 mM), $MgCl_2$ (30

Table 3. Regioselectivity of Testosterone and AFB_1 Hydroxylations by P450s 3A4 and Its Structural Mutants

	testosterone (T) hydroxylation[a] (nmol OH-T formed/nmol P450/min)			AFB_1 hydroxylation[b] (nmol AFB_1 metabolite formed/nmol P450/min)		
P450s	6β-OHT	2β-OHT	6β-/2β-OHT	AFQ_1	8,9-epoxide	AFQ_1/8,9-epoxide
3A4wt	28.4 ± 2.57	2.21 ± 0.14	12.9	2.63 ± 0.04	1.07 ± 0.02	2.43
N206S	1.86 ± 0.52	ND[c]		0.12 ± 0.07	0.38 ± 0.05	0.31
N206E	21.9 ± 1.01	3.41 ± 0.18	6.43	0.77 ± 0.01	0.36 ± 0.05	2.01
E244A	19.6 ± 5.38	1.69 ± 0.08	11.6	1.08 ± 0.14	0.43 ± 0.00	2.52
E244V	37.6 ± 7.23	6.50 ± 1.17	5.78	0.85 ± 0.03	0.50 ± 0.08	1.70
E244N	18.3 ± 3.76	1.12 ± 0.05	16.3	1.08 ± 0.08	0.44 ± 0.08	2.45
E244S	28.2 ± 3.43	7.05 ± 1.07	4.0	0.55 ± 0.12	0.35 ± 0.07	1.57
N206E/E244N	8.32 ± 0.08	0.97 ± 0.04	8.62	0.05 ± 0.01	0.10 ± 0.02	0.50
F304A	15.1 ± 0.65	ND		ND	ND	

[a] Values listed are mean ± SD of at least three individual determinations. [b] AFQ_1 is the 3α-hydroxylated AFB_1 metabolite. 8,9-Epoxides were assayed by the combined yield of their GSH adducts and the diol species. Values listed are the mean ± SD of at least four individual determinations. [c] ND, nondetectable.

mM), AFB_1 (50 μM in 5 mL of methanol), purified rat liver GSH *S*-transferase (0.2 mg/mL) and NADPH (1 mM) in a final volume of 0.5 mL. The final concentration of CHAPS in the incubations was limited to 0.2%, to prevent the functional inhibition observed at higher concentrations. The reaction was initiated by the addition of NADPH and stopped by the addition of 25 μL of 1.47 M formic acid after incubation with shaking (200 rpm) for 20 min at 37 °C. After vortexing, the protein was pelleted by centrifugation and the supernatant was filtered through a Nylon membrane filter (Rainin Nylon-66, 0.45 mm pore size) and analyzed by HPLC as described previously (*23*). Metabolites were characterized by comparison to authentic synthetic standards and quantified by integration of peak areas as described previously (*23*). In assays carried out to examine the homotropic interactions of AFB_1 with P450 3A4 or its N206S mutant, the AFB_1 concentrations were varied between 0 and 100 μM in otherwise identical incubation systems. The data from these assays were analyzed by standard Hill plot kinetics as described previously (*9*).

Computer Modeling of P450 3A4. Molecular modeling was performed on a Silicon Graphics workstation using InsightII/Discover_3 software package (MSI, San Diego, CA). The crystal structure of AFB_1 was obtained earlier from the Cambridge Structural Database (*23*). Initial experiments were carried out with the previously reported P450 3A4 homology model (*29*), using the conditions previously described (*23*).

The P450 3A4 structure was refined from the previous version (*29*) by realignment of the F-helix and B′-helix using Homology and Biopolymer modules of InsightII. The segment from position 197 to 228 (including the F-helix) of P450 3A4 was moved four residues forward, and the segment from position 103 to 115 (including the B′-helix) was moved two residues backward. In the new alignment, Leu211 in the F-helix of P450 3A4 now corresponds to the active-site residues Thr185 in P450101 and Leu175 in P450107. Phe108 in the B′-helix of P450 3A4 corresponds to the active-site residue Phe78 in P450107. The coordinates of the F-helix (residues 202−219) were then assigned based on the average coordinates of the four P450 bacterial structures, P450s 101, 102, 107, and 108. The loops before and after the F-helix (residues 197−201 and residues 220−228) were generated with Homology using a random tweak algorithm. For the B′-helix (residues 108−115), the coordinates were assigned based only on P450107. The loops before and after B′-helix (residues 103−107 and residues 116−123) were also generated. The coordinates of the other regions of P450 3A4 were unchanged from the previous model (*29*).

After coordinate assignment, the preliminary 3D structure of P450 3A4 was refined. Energy minimization was performed by Discover-3/InsightII using a consistent valence force field. The parameters for the heme group were those described previously (*23*, *29*). In the first step of structural refinement, the splice regions between residues 102 and 103, 107 and 108, 115 and 116, 123 and 124, 196 and 197, 201 and 202, 219 and 220, and 228 and 229 were repaired by Homology/InsightII to avoid steric hindrance in these junction regions. Then all newly generated loops were optimized using molecular dynamics followed by energy minimization. The model was then subjected to minimization on the whole structure. First, all hydrogen atoms of the P450 3A4 enzyme were minimized, while heavy atoms were kept fixed. Then, side chains were minimized with the backbone fixed. This was followed by the minimization of the structure after soaking it with water using a sphere of 25 Å and a layer of 3 Å. Protein-water association was then minimized with conjugate gradients to a maximum of 1 kcal mol^{-1} $Å^{-1}$.

AFB_1 was automatically docked into the refined 3A4 model with the Affinity module of InsightII (MSI, San Diego). One AFB_1 molecule was docked into the active site in an orientation leading either to 3α-hydroxylation or *exo*-8,9-epoxidation. Then, a second AFB_1 molecule was also automatically docked into the active site in the presence of the first one at either 3α-hydroxylation or *exo*-8,9-epoxide binding orientation.

Results and Discussion

Relative Functional Activities of P450 3A4 SRS-2 Mutants. The values for testosterone 6β- and 2β-hydroxylase and AFB_1 3α-hydroxylase and *exo*-8,9 epoxidase activities of wild-type P450s 3A4 and 3A5 have been reported previously (*23*). Substitution of N206 in the P450 3A4 SRS-2 region with Ser resulted in marked decreases of all these activities in confirmation of our previous findings (Table 2), with the rates of AFB_1 metabolite formation and the AFQ_1/8,9-epoxide ratio closely mimicking those of P450 3A5 wild-type. Replacement of L210 in the P450 3A4 SRS-2 region with Phe, on the other hand, had little effect on the extent or regioselectivity of testosterone hydroxylation but markedly decreased AFB_1 hydroxylation with the rates of AFB_1 metabolite formation and the AFQ_1/8,9-epoxide ratio closely mimicking those of N206S and P450 3A5 wild-type, as shown previously. Substitution of Leu210 with Ala (L210A) affected testosterone 2β-hydroxylation but not its 6β-hydroxylation, in confirmation of previous findings (*10*). The L210A mutant also exhibited markedly reduced AFB_1 3α-hydroxylase activity with *exo*-8,9-epoxidase activity comparable to that of the other two SRS-2 mutants, N206S and L210F (Table 2). Replacement of SRS-2 residue L211 with Phe generated a mutant capable of efficient testosterone 6β-hydroxylation and even somewhat enhanced testosterone 2β-hydroxylation, consistent with a previous report (*11*), but its AFB_1 3α-hydroxylase appeared to be selectively decreased with little effect on its *exo*-8,9-epoxidase activity relative to the P450 3A4 wild-type AFB_1 oxidase activities. Substitution of L211 with the smaller Ala residue, on the other hand, reduced all four activities, thereby revealing the

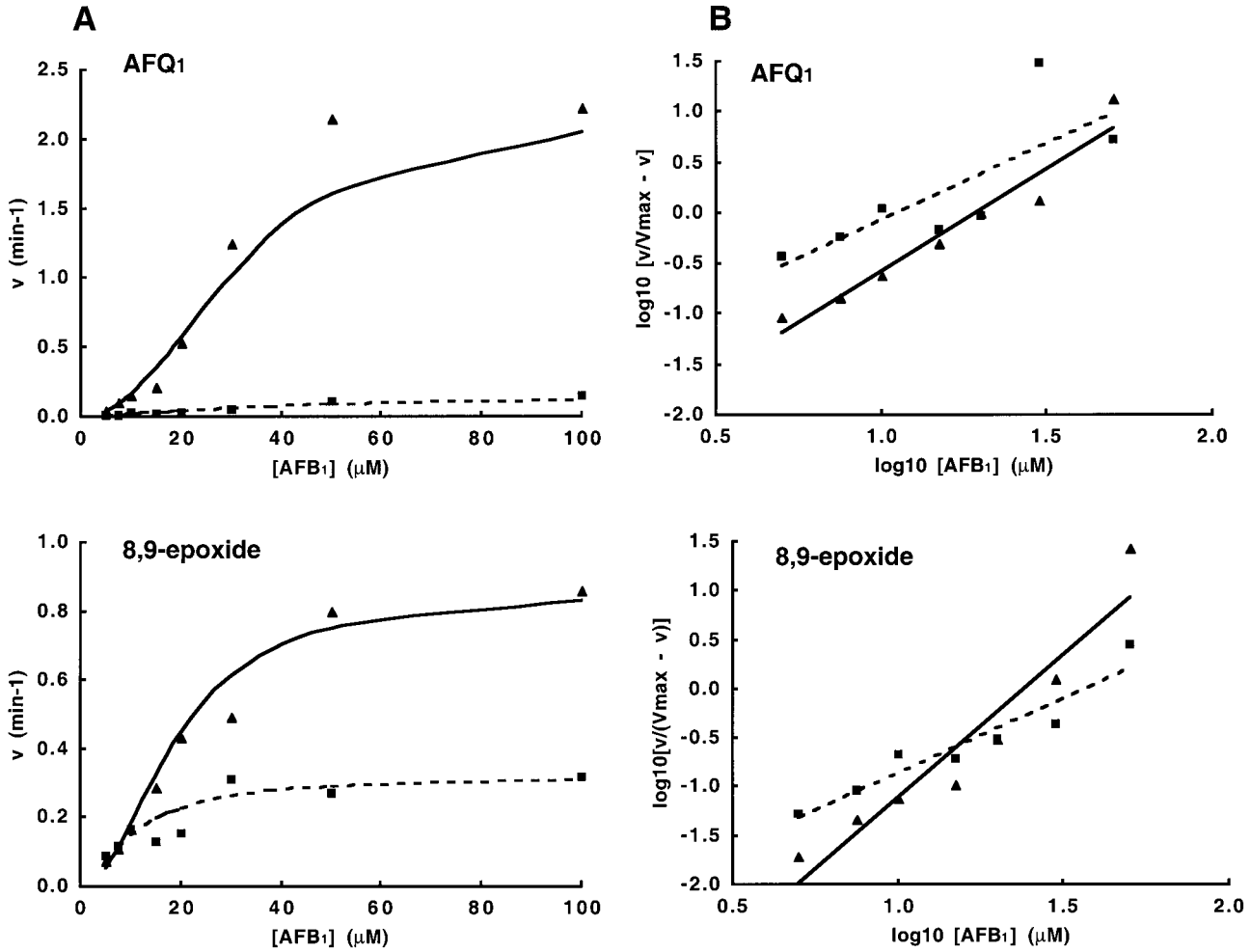

Figure 1. Kinetic analyses of AFB_1 3α-hydroxylation and *exo*-8,9-epoxidation catalyzed by P450 3A4 wild-type and its N206S mutant. AFB_1 metabolism was determined as described (Experimental Procedures). The values plotted are averages of two individual determinations (panel A). The corresponding Kcat values (min^{-1}) for P450 3A4 wild-type and N206S mutant were 2.23 and 0.15 nmol of 3α-hydroxylated AFB_1 metabolite (AFQ_1), respectively, and 0.86 and 0.32 nmol of AFB_1 *exo*-8,9-epoxide, respectively. Solid lines and triangles correspond to P450 3A4 wild-type values and the dashed lines and solid squares to those of the N206S mutant, respectively. Their AFQ_1 and AFB_1 8,9-epoxide formation are depicted in the top and bottom parts of panel A, respectively. The corresponding results fitted to plots of log $[v/(V_{max} - v)]$ vs log AFB_1 (μM) are depicted in the top and bottom parts of panel B, respectively. The *n* values are given in the text.

importance of this or a residue of equivalent bulk or hydrophobicity for P450 3A4 catalyses. Interestingly, the double mutant N206S/K209M was incapable of either testosterone 6β- or 2β-hydroxylation or of AFB_1 3α-hydroxylation but was highly active in AFB_1 *exo*-8,9-oxidation, thereby converting P450 3A4 into a catalyst predominantly committed to the AFB_1 genotoxic pathway. Together these findings attest to the critical importance of several P450 3A4 SRS-2 residues in AFB_1 oxidation, particularly for its 3α-hydroxylase detoxification pathway.

Relative AFB_1 Homotropic Interactions of P450 3A4 Wild-Type (wt) and Its N206S Mutant. The above findings obtained at concentrations of testosterone (0.25 mM) and AFB_1 (50 μM) known to elicit maximal *homotropic substrate interactions* (*9*−*11*) revealed that mutations of certain residues in the P450 3A4 SRS-2 domain differentially affected the metabolism of the two substrates, with marked impairment of AFB_1 metabolism observed with mutants L210F, L210A, L211F, and L211A. Replacement of L210 and L211 with Ala or Phe is also known to diminish the α-naphthoflavone (ANF)-induced heterotropic stimulation of testosterone hydroxylation, in some instances by raising the basal activities (*10*, *11*) at subsaturating steroid concentrations. N206S on the other hand, exhibited considerably decreased metabolism of both substrates, thereby revealing the critical role of N206 in P450 3A4 catalysis. To determine whether impaired AFB_1 metabolism by N206S reflected altered AFB_1 cooperativity (*9*, *28*), the kinetics of its AFB_1 3α-hydroxylase and *exo*-8,9-epoxidase activities were compared with those of P450 3A4wt at AFB_1 concentrations ranging from 0 to 100 μM. Graphic plots (*v* vs *S*) of these kinetic data revealed that while P450 3A4wt yielded the expected sigmoidal curve profiles for both activities previously reported (*9*, *28*), N206S yielded profiles that could not be classified as sigmoidal (Figure 1). Corresponding plots of Hill transformations of these data revealed that N206S mutation did indeed lower the Hill coefficients for AFB_1 3α-hydroxylation and *exo*-8,9-oxidation, from $n = 2.9$ and 2.0 for P450 3A4wt to $n = 1.5$ and 1.5, respectively. The finding of a Hill coefficient of $n = 2.9$ for AFB_1 3α-hydroxylation is entirely consistent with the triple substrate occupancy previously proposed for the wild-type enzyme (*8*, *14*). However, the lowering of this *n* value to 1.5 suggests that the introduction of

the S206 residue in the 3A4 active site affects the ability of the enzyme to bind more than one substrate molecule and consequently its sigmoidal Hill kinetics with a rather dramatic reduction of its AFB_1 3α-hydroxylase activity (Figure 1).

Potential Explanations for the Relative Functional Inactivity of N206S Mutant from P450 3A4 Molecular Modeling Analyses and Their Empirical Validation through Site-Directed Mutagenesis and Functional Assays. In the absence of a P450 3A4-AFB_1 crystal structure that could explain this finding, we sought insight into it by computer docking AFB_1 into the active site of a previously described P450 3A4 homology model (*29*). Molecular dynamics analyses suggested that the side chain NH_2 group of N206 may form H-bonds with the carboxyl group of E244, thereby creating a salt bridge that stabilizes the protein structure and/or defines the active site cavity through interactions between helix F (N206) and helix G (E244). To test the validity of these analyses, we generated several additional P450 3A4 mutants (E244A, E244N, E244S, E244V, and N206E), with the specific intention of either disrupting this N206-E244 H-bond or restructuring this H-bond through a N206E/E244N double mutation (Table 3). All of these mutants were heterologously expressed in *E. coli* as structurally and functionally intact hemoproteins. E244A and E244N exhibited comparable impairment of AFB_1 3α-hydroxylation (AFQ_1 formation) and *exo*-8,9-oxidation, with little consequent influence on the AFQ_1/epoxide formation ratio (∼2.45). The AFB_1 3α-hydroxylation of E244V and E244S was lowered to a slightly greater extent than their *exo*-8,9-epoxidation, with consequently lowered AFQ_1/epoxide ratios. These findings thus reveal differences in the relative importance of the E244 residue for each AFB_1 orientation within the active site, with AFB_1 3α-hydroxylation being the most affected by substitution of E244 with Ser. The Glu substitution at N206 on the other hand, affected AFQ_1 formation to a slightly greater extent than *exo*-8,9-oxidation yielding an AFQ_1/epoxide ratio of ∼2.0, but the resulting protein still retained appreciable AFB_1 3α-hydroxylase activity relative to N206S (AFQ_1/epoxide ratio of ∼0.31). Furthermore, our attempted restructure of the H-bond through N206E/E244N created an enzyme that was relatively inactive in both pathways, with an AFQ_1/epoxide ratio of 0.5, thereby revealing the importance of Asn and Glu in those precise active site positions (N206 and E244). It is noteworthy that these mutations (with the notable exception of N206E/E244N) had a significantly lesser effect on testosterone hydroxylation. Indeed, mutants E244V and E244S, if at all, exhibited enhanced regioselectivity toward 2*β*-hydroxylation (Table 3). The finding that replacement of certain P450 3A4 residues had quantitatively and/or qualitatively different effects on the two substrates, testosterone and AFB_1, once again underscores the uniqueness of each P450 3A4 substrate-active site fit.

AFB_1 Docking Analyses in a Refined P450 3A4 Model. The above empirically obtained data thus failed to validate the predictions of a H-bond between N206 and E244 derived from AFB_1 molecular modeling analyses with the existing P450 3A4 homology model (*29*). Recent discovery of similar discrepancies between empirically derived observations[3] and predictions from molecular modeling with the existing P450 3A4 homology model (*29*), coupled with newly acquired insight from the only mammalian liver P450 X-ray crystal structure reported to date (*30*), has led to the refinement of the P450 3A4 homology model to be described in greater detail elsewhere.[4] Such refinement specifically entails a realignment of the P450 3A4 F-helix by one helical turn such that residue L211 (rather than F215) now aligns with Thr185 of P450101 and Leu175 of P450107, as well as a realignment of the B′-helix. Thus, this F-helix realignment would directly influence the relative positioning within the P450 3A4 active site of SRS-2 residues at positions 206, 210, and 211 examined in this study (Table 2), with consequently profound implications for any analyses of the corresponding mutants. As such, because of the questionable validity of any structural/functional interpretations derived from analyses of these residues with the older P450 3A4 homology model (*29*), we have reassessed the relative role of SRS-2 residues by computer docking analyses of AFB_1 in the refined P450 3A4 homology model with the realigned F-helix. In this context, it is noteworthy that the F-helix region of P450s is widely recognized to be not only highly variable in length and amino acid sequence, but also susceptible to considerable shifts induced by substrate binding (*16*, *31*).

(1) AFB_1 Docking within P450 3A4 Active Site in an Orientation Leading to 3α-Hydroxylation. Two AFB_1 molecules could be autodocked within the active site of the refined P450 3A4 model, with the first molecule bound in an orientation conducive to 3α-hydroxylation and thus in a "*substrate*" binding mode, and the second in the "*activator/effector*" mode (*23*). In this docking mode, N206 appeared to be sufficiently close to the phenyl group of F304 to enable interactions between the two side chains (Figure 2). Substitution of N206 to residues such as Ser could affect these interactions and consequently the position of the phenyl group of F304 relative to AFB_1 substrate and hence AFB_1 3α-hydroxylation. In this refined model, L210 appears to be near both AFB_1 molecules, whereas L211 is apparently proximal to the activator AFB_1 molecule. Replacement of each of these residues could affect the docking of both molecules in the active site, as Leu at each of these positions allows an optimal fit of both molecules within the cavity. Thus, substitution with residues larger or smaller than Leu could unfavorably alter this AFB_1 active site fit and AFB_1 homotropic interactions, and consequently impair AFB_1 3α-hydroxylation.

(2) AFB_1 Docking within P450 3A4 Active Site in an Orientation Leading to *exo*-8,9-Epoxidation. As previously, AFB_1 can only be docked in an orientation conducive to *exo*-, but not *endo*-8,9-epoxidation (*23*; Figure 3). In this AFB_1 orientation, a relatively strong pi−pi interaction between the phenyl group of F304 and the aromatic ring system of the AFB_1 substrate molecule apparently occurs. Substitution of N206 with Ser apparently alters the interaction between residue 206 and the F304 phenyl group, but not sufficiently to markedly affect the pi−pi interactions between F304 phenyl and the AFB_1 aromatic ring system. This possibility is consistent with the observed very modest impairment of AFB_1 *exo*-8,9 epoxidation in functional assays of the N206S mutant relative to that of the wild-type enzyme (Table 2).

[3] Halpert and co-workers, unpublished observations.

[4] Halpert and co-workers, manuscript in preparation.

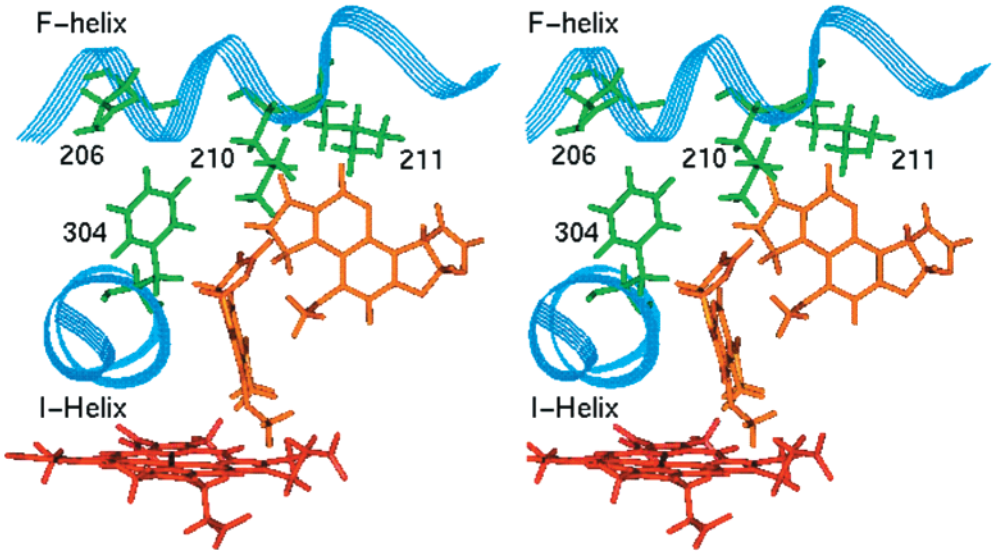

Figure 2. AFB_1 docked into the active site of the refined P450 3A4 model in an orientation conducive to its 3α-hydroxylation. A second AFB_1 molecule (activator) is also shown making contacts with residues L210 and L211 of the F-helix.

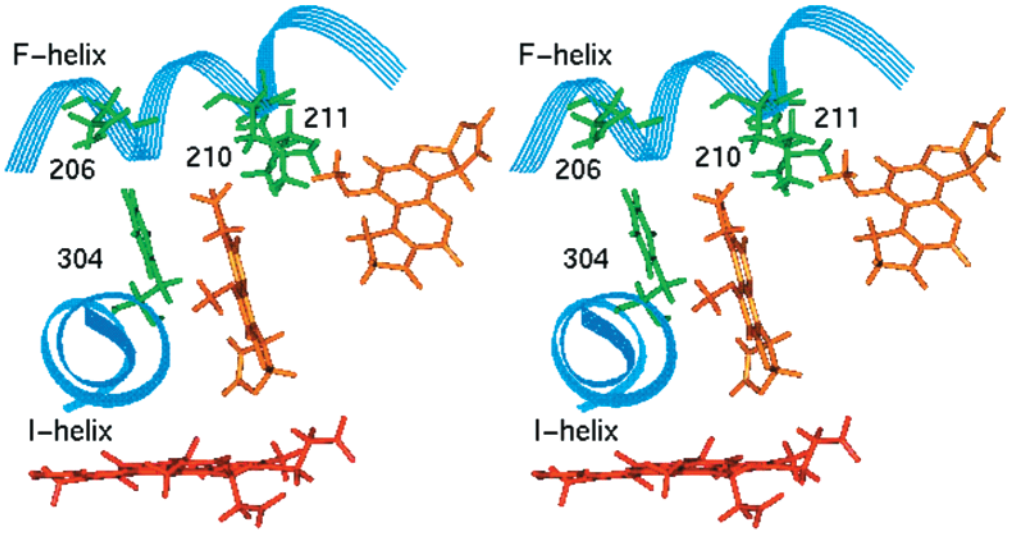

Figure 3. AFB_1 docked into the active site of the refined P450 3A4 model in an orientation conducive to its *exo*-8,9-epoxidation. A second AFB_1 molecule (activator) is also shown making contacts with residue L211 of the F-helix.

Similarly, substitution of residue L210 and L211 with Phe or Ala resulted in comparable effects on AFB_1 *exo*-8,9 epoxidation as those observed with N206S mutant, thereby suggesting that a pi−pi interaction involving residue F304 may be strong enough on its own, requiring only minor assistance from the neighboring 206, 210, and 211 residues to maintain the two AFB_1 molecules in an orientation conducive to *exo*-8,9 epoxidation of the AFB_1 substrate molecule.

Role of F304 in P450 3A4-Catalyzed AFB_1 Oxidation. On the basis of P450 3A4 amino acid sequence alignment with those of bacterial P450s with known crystal structures, F304 is believed to lie in the highly conserved I-helix, which contains several residues proposed to be key substrate contact points (*16*, *32*−*35*). In particular, residue F304 is proposed to play a pivotal role in the homotropic and heterotropic P450 3A4−substrate interactions, given that in conjunction with other active site residues (L211 and D214) it may provide important contacts for both substrate and effector (activator) molecules within the P450 3A4 active site (*12*, *16*). To determine whether F304 was indeed relevant to P450 3A4 catalyzed AFB_1 oxidation, as predicted from our molecular modeling analyses, we examined the functional activity of the F304A mutant. Indeed as predicted from these analyses, replacement of F304 with Ala, completely abolished both AFB_1 3α-hydroxylation as well as AFB_1 *exo*-8,9-epoxidation (Table 3). These findings are entirely consistent with the apparently pivotal role of F304 on one hand, in anchoring AFB_1 in orientations conducive to 3α-hydroxylation and *exo*-8,9-epoxidation potentially through van der Waals interactions and pi−pi interactions, respectively, while on the other hand, maintaining the active site architecture through its putative interactions with N206. Thus, not surprisingly, any disruption of this structural framework, through substitutions of either F304 or even N206, could result in a P450 3A4 enzyme that is either completely inactive (F304A) or

[5] Preliminary findings indicate that the AFB_1 oxidation activities of the K209M mutant are nearly comparable to those of the wild-type enzyme.

[6] Eiselt et al., Pharmacogenetics, in press, 2001.

functionally sluggish (N206S). The relatively lowered, albeit significant, testosterone 6β-hydroxylase activity of F304 mutant relative to that of the wild-type is consistent with previous reports (*12*) and confirms that the loss of its AFB_1 oxidation activities is not due to global loss of function, but selective to AFB_1 as the substrate. These findings once again emphasize the uniqueness of each P450 3A4 substrate−active site interactions. On the basis of these analyses, it is plausible that other P450 3A4 residues of the I-helix such as I301 and A305 may also influence the AFB_1−active site interaction. Indeed, mutation of A305 to Phe or Ser has been recently shown to affect the oxidation of several P450 3A4 substrates (diazepam, erythromycin, nifedipine, and testosterone) and/or impair the binding of azole inhibitors to the P450 3A4 heme iron (*36*).

Conclusions. The above findings clearly underscore the functional differences between the two human liver P450s 3A and indicate that a single residue in a single SRS region (SRS-2 or SRS-4) can profoundly alter the catalytic function of the enzymes and consequently the metabolic pathways of drugs and other chemicals, thereby influencing their relative partitioning through toxic vs nontoxic pathways. Accordingly, P450 3A4, an enzyme that is predominantly detoxifying for a hepatotoxin such as AFB_1, can through a single substitution (N206S) be converted to a largely toxifying entity. This property is further enhanced with the additional K209M mutation.[5] On the other hand, mutation of the SRS-4 residue F304 can totally abolish AFB_1 metabolism. These findings with AFB_1 as a probe have a direct bearing for single allelic variants of the P450 3A4 gene (*known and yet to be discovered*) in the human population that may result in function polymorphisms and consequent alterations of P450 3A4-dependent metabolic pathways of clinically relevant drugs as well as other xenobiotics. Recently, variant alleles of P450 3A4 gene representing the very first examples of potential human function polymorphisms have been identified. One of these variant alleles (P450 3A4*2) found in 2.7% of the white population, expressed a P450 3A4S222P mutant enzyme exhibiting impaired metabolism of the Ca^{2+} blocker nifedipine, relative to that of the wild-type (*37*). Another P450 3A4 variant allele expressed a protein with a L373F mutation with functional properties considerably different from those of the wild-type enzyme.[6] The identification of such function polymorphisms in the human population however, underscores the clinical relevance of examining structure−function relationships of these important human enzymes and reveals that a single amino acid divergence can profoundly influence function, with consequent alterations in drug disposition and clinical/toxic outcome. Furthermore, in individuals representing 25−30% of the human population that express P450 3A5 as their predominant if not sole isoform, such functional differences not only may directly influence their relative susceptibility to AFB_1 genotoxicity, but also may directly impact on the clinical efficacy and drug−drug interactions of chloramphenicol, quinidine and cyclosporine A, drugs that are differentially metabolized by this isoform.

Acknowledgment. The authors sincerely thank Prof. R. W. Estabrook (University of Texas, Southwestern Medical School, Dallas, TX) for the P450 3A4 and P450 3A5 plasmids, Prof. T. M. Harris (Vanderbilt University, Nashville, TN) for the gift of AFB_1 *exo*-8,9-oxide, Dr. Greg Harlow (Selectide, Tucson, AZ) who provided the plasmids for the expression of the P450 3A4 L210 and L211 mutants, and Ryan Dick for the N206S plasmid. They also thank Dr. Deanna Kroetz (University of California, San Francisco) for valuable discussions on the methodology used, and Dr. Bernard Murray (University of California, San Francisco) for AFB_1 docking analyses with RasMol and assistance with enzyme kinetics. The authors wish to acknowledge the UCSF Liver Center Core Facility on Molecular Analyses (Spectrophotometry Component, supported by NIDDKD 26743), and the West Virginia University Computational Chemistry and Molecular Modeling Laboratory. This research project was supported by USPHS grants DK26506 (M.A.C.), CA85542 (G.D.S.), GM54995 (J.R.H.), and ES06676 (University of Texas Medical Branch) as well as by West Virginia University Senate Research Grant (G.D.S.).

References

(1) Guengerich, F. P. (1987) *Mammalian Cytochromes P450*, Vol. I and II, CRC Press, Boca Raton, FL.

(2) Ortiz de Montellano, P. R. (1995) In *Cytochrome P450: Structure, Mechanism and Biochemistry* (Ortiz de Montellano, P. R., Ed.) pp 473−574, Plenum Press, New York.

(3) Correia, M. A. (2001) Drug Biotransformation. In *Basic and Clinical Pharmacology* (Katzung, B. G., Ed.) 8th ed., Chapter 5, pp 51−63, Appleton & Lange, San Mateo.

(4) Wrighton, S. A., and Stevens, J. C. (1992) The human hepatic cytochromes P450 involved in drug metabolism. *Crit. Rev. Toxicol.* **22**, 1−21.

(5) Guengerich, F. P. (1995) Human cytochrome P450 enzymes. In *Cytochrome P450: Structure, Mechanism and Biochemistry* (Ortiz de Montellano, P. R., Ed.) pp 473−574, Plenum Press, New York.

(6) Thummel, K. E., and Wilkinson, G. R. (1998) In vitro and in vivo drug interactions involving human P450 3A. *Annu. Rev. Pharmacol. Toxicol.* **38**, 389−430.

(7) Guengerich, F. P. (1999) Cytochrome P450 3A4: Regulation and role in drug metabolism. *Annu. Rev. Pharmacol. Toxicol.* **39**, 1−17.

(8) Shou, M., Grogan, J., Mancewicz, J. A., Krausz, K. W., Gonzalez, F. J., Gelboin, H. V., and Korzekwa, K. R. (1994) Activation of P450 3A4: evidence for the simultaneous binding of two substrates in a cytochrome P450 active site. *Biochemistry* **33**, 6450−6455.

(9) Ueng, Y. F., Kuwabara, T., Chun, Y.-J., and Guengerich, F. P. (1997) Cooperativity in oxidations catalyzed by cytochrome P450 3A4. *Biochemistry* **36**, 370−381.

(10) Harlow, G. R., and Halpert, J. R. (1997) Alanine-scanning mutagenesis of a putative substrate recognition site in human cytochrome P450 3A4. Role of residues 210 and 211 in flavonoid activation and substrate specificity. *J. Biol. Chem.* **272**, 5396−5402.

(11) Harlow, G. R., and Halpert, J. R. (1998) Analysis of human cytochrome P450 3A4 cooperativity: construction and characterization of a site-directed mutant that displays hyperbolic steroid hydroxylation kinetics. *Proc. Natl. Acad. Sci. U.S.A.* **95**, 6636−6641.

(12) Domanski, T. L., Liu, J., Harlow, G. R., and Halpert, J. R. (1998) Analysis of four residues within substrate recognition site 4 of human cytochrome P450 3A4: role in steroid hydroxylase activity and alpha-naphthoflavone stimulation. *Arch. Biochem. Biophys.* **350**, 223−232.

(13) Korzekwa, K. R., Krishnamachary, N., Shou, M., Ogai, A., Parise, R. A., Rettie, A. E., Gonzalez, F. J., and Tracy, T. S. (1998) Evaluation of atypical cytochrome P450 kinetics with two-substrate models: evidence that multiple substrates can simultaneously bind to cytochrome P450 active sites. *Biochemistry* **37**, 4137−4147.

(14) Hosea, N. A., Miller, G. P., and Guengerich, F. P. (2000) Elucidation of distinct ligand binding sites for cytochrome P450 3A4. *Biochemistry* **39**, 5929−5939.

(15) Shou, M., Mei, Q., Ettore, M. W., Jr., Dai, R., Baillie, T. A., and Rushmore, T. H. (1999) Sigmoidal kinetic model for two cooperative substrate-binding sites in a cytochrome P450 3A4 active site: an example of the metabolism of diazepam and its derivatives. *Biochem. J.* **340**, 845−853.

(16) Domanski, T. L., He, Y. A., Harlow, G. R., and Halpert, J. R. (2000) Dual role of human cytochrome P450 3A4 residue Phe-

304 in substrate specificity and cooperativity. *J. Pharmacol. Exp. Ther.* **293**, 585−591.
(17) Wrighton, S. A., Ring, B. J., Watkins, P. B., and VandenBranden, M. (1989) Identification of a polymorphically expressed member of the human cytochrome P-450III family. *Mol. Pharmacol.* **36**, 97−105.
(18) Wrighton, S. A., Brian, W. R., Sari, M.-A., Iwasaki, M., Guengerich, F. P., Raucy, J. L., Molowa, D. T., and Vandenbranden, M. (1990) Studies on the expression and metabolic capabilities of human liver cytochrome P450IIIA5 (HLp3). *Mol. Pharmacol.* **38**, 207−213.
(19) Aoyama, T., Yamano, S., Waxman, D. J., Lapenson, D. P., Meyer, U. A., Fischer, V., Tyndale, R., Inaba, T., Kalow, W., Gelboin, H. V., and Gonzalez, F. J. (1989) Cytochrome P-450 hPCN3, a novel cytochrome P-450 IIIA gene product that is differentially expressed in adult human liver. cDNA and deduced amino acid sequence and distinct specificities of cDNA-expressed hPCN1 and hPCN3 for the metabolism of steroid hormones and cyclosporine. *J. Biol. Chem.* **264**, 10388−10395.
(20) Gillam, E. M., Baba, T., Kim, B. R., Ohmori, S., and Guengerich, F. P. (1993) Expression of modified human cytochrome P450 3A4 in *Escherichia coli* and purification and reconstitution of the enzyme. *Arch. Biochem. Biophys.* **305**, 123−131.
(21) Gillam, E. M., Guo, Z., Ueng, Y. F., Yamazaki, H., Cock, I., Reilly, P. E., Hooper, W. D., and Guengerich, F. P. (1995) Expression of cytochrome P450 3A5 in *Escherichia coli*: effects of 5′ modification, purification, spectral characterization, reconstitution conditions, and catalytic activities. *Arch. Biochem. Biophys.* **317**, 374−384.
(22) Gallagher, E. P., Wienkers, L. C., Stapleton, P. L., Kunze, K. L., and Eaton, D. L. (1994) Role of human microsomal and human complementary DNA-expressed cytochromes P4501A2 and P450 3A4 in the bioactivation of aflatoxin B1. *Cancer Res.* **54**, 101−108.
(23) Wang, H., Dick, R., Yin, H., Licad-Coles, E., Kroetz, D., Szklarz, G., Halpert, J. R., and Correia, M. A. (1998) Structure−Function Relationships of Human Liver Cytochromes P450 3A: Aflatoxin B_1 Metabolism as a Probe. *Biochemistry* **37**, 12536−12545.
(24) Licad-Coles, E., He, K., Yin, H., and Correia, M. A. (1997) Cytochrome P450 2C11: *Escherichia coli* expression, purification, functional characterization, and mechanism-based inactivation of the enzyme. *Arch. Biochem. Biophys.* **338**, 35−42.
(25) Raney, K. D., Shimada, T., Kim, D. H., Groopman, J. D., Harris, T. M., and Guengerich, F. P. (1992) Oxidation of aflatoxins and sterigmatocystin by human liver microsomes: significance of aflatoxin Q_1 as a detoxication product of aflatoxin B_1. *Chem. Res. Toxicol.* **5**, 202−210.
(26) Omura, T., and Sato, R. (1964) The carbon monoxide-binding pigment of liver microsomes. I. Evidence for its hemoprotein nature. *J. Biol. Chem.* **239**, 2370−2378.
(27) Underwood, M. C., Cashman, J. R., and Correia, M. A. (1992) Specifically designed thiosteroids as active-site-directed probes for functional dissection of rat liver cytochrome P450 3A isozymes. *Chem. Res. Toxicol.* **5**, 42−53.
(28) Ueng, Y. F., Shimada, T., Yamazaki, H., and Guengerich, F. P. (1995) Oxidation of aflatoxin B1 by bacterial recombinant human cytochrome P450 enzymes. *Chem. Res. Toxicol.* **8**, 218−225.
(29) Szklarz, G. D., and Halpert, J. R. (1997) Molecular modeling of cytochrome P450 3A4. *J. Comput. Aided Mol. Des.* **11**, 265−272.
(30) Williams, P. A., Cosme, J., Sridhar, V., Johnson, E. F., and McRee, D. E. (2000) Mammalian microsomal cytochrome P450 monooxygenase: structural adaptations for membrane binding and functional diversity. *Mol. Cell* **5**, 121−131.
(31) Modi, S., Sutcliffe, M. J., Primrose, W. U., Lian, L. Y., and Roberts, G. C. (1996) The catalytic mechanism of cytochrome P450 BM3 involves a 6 A movement of the bound substrate on reduction. *Nat. Struct. Biol.* **3**, 414−417.
(32) Gotoh, O. (1992) Substrate recognition sites in cytochrome P450 family 2 (P4502) proteins inferred from comparative analyses of amino acid and coding nucleotide sequences. *J. Biol. Chem.* **267**, 83−90.
(33) Hasemann, C. A., Kurumbail, R. G., Boddupalli, S. S., Peterson, J. A., and Deisenhofer, J. (1995) Structure and function of cytochromes P450: a comparative analysis of three crystal structures. *Structure* **3**, 41−62.
(34) Nelson, D. R. (1995) Cytochrome P450 nomenclatures and alignment of selected sequences. In *Cytochrome P450: Structure, Mechanism and Biochemistry* (Ortiz de Montellano, P. R., Ed.) pp 575−606, Plenum Press, New York.
(35) von Wachenfeldt, C., and Johnson, E. F. (1995) Structures of eukaryotic cytochrome P450 enzymes. In *Cytochrome P450: Structure, Mechanism and Biochemistry* (Ortiz de Montellano, P. R., Ed.) pp 183−223, Plenum Press, New York.
(36) Fowler, S. M., Riley, R. J., Pritchard, M. P., Sutcliffe, M. J., Friedberg, T., and Wolf, C. R. (2000) Amino acid 305 determines catalytic center accessibility in P450 3A4. *Biochemistry* **39**, 4406−4414.
(37) Sata, F., Sapone, A., Elizondo, G., Stocker, P., Miller, V. P., Zheng, W., Raunio, H., Crespi, C. L., and Gonzalez, F. J. (2000) P450 3A4 allelic variants with amino acid substitutions in exons 7 and 12: evidence for an allelic variant with altered catalytic activity. *Clin. Pharmacol. Ther.* **67**, 48−56.

TX000218Z